

# Extraction of Negative Hydrogen Ions using a Plasma Electrode Covered by Ta or Ti

K. Maeshiro<sup>1, a)</sup>, M. Wada<sup>1, b)</sup> and S. Masaki<sup>2</sup>

<sup>1</sup>Graduate School of Science and Engineering, Doshisha University, Kyoto, 610-0394, Japan

<sup>2</sup>Department of Fusion Science, The Graduate University for Advanced Studies, SOKENDAI, Toki, Gifu 509-5292, Japan

<sup>a)</sup>Corresponding author: ctwd0333@mail4.doshisha.ac.jp

<sup>b)</sup>[mwada@mail.doshisha.ac.jp](mailto:mwada@mail.doshisha.ac.jp)

**Abstract.** We compared the effect of a tantalum (Ta) fresh coating with that of a Ta thin sheet covering the plasma electrode of a negative hydrogen ion source on the ratio of extracted negative hydrogen ( $H^-$ ) ion current to extracted electron current. Fresh Ta evaporation from a thin hot Ta filament showed about 22 % increase of extracted  $H^-$  ion current compared to the operation with tungsten (W) hot filament. On the other hand, a thin Ta foil covering the plasma electrode decreased the extracted electron current without any large influence on  $H^-$  ion current. Meanwhile, when a titanium (Ti) foil covered the plasma electrode, both the extracted  $H^-$  ion current and electron current decreased substantially. At a plasma electrode bias higher than the plasma potential, the ratio of  $H^-$  ion current to the electron current for the Ti covered plasma electrode exceeded 80%.

## INTRODUCTION

Neutral beam injection (NBI) heating requires a negative hydrogen ( $H^-$ ) ion beam since the neutralization efficiency at higher beam energy becomes negligible for a positive hydrogen ion beam [1]. It is common to deposit cesium (Cs) on the plasma electrode surface as a method for improving  $H^-$  ion production efficiency and reduce co-extracted electron current [2]. However, introducing Cs to an  $H^-$  source can cause Cs leakage to high voltage holding system of the accelerator leading to a breakdown. Thus, the use of Cs is preferred to be avoided and materials which could be used to realize Cs-free ion source operation are currently investigated [3,4]. Source operation with tantalum (Ta) filaments as the arc discharge cathode is known to increase the production of negative hydrogen ions while reducing the co-extracted electron current [5,6]. High-temperature cathode filaments made of Ta as compared to tungsten (W), may improve the production rate of hydrogen vibrationally excited molecules ( $H_2^*$ ) and thus that of  $H^-$  ions in a hydrogen plasma [7]. There is another possible explanation of the observed enhanced  $H^-$  ion production. A plasma electrode coated with Ta may efficiently absorb hydrogen atoms which destroy the hydrogen negative ions by associative detachment [8]. Meanwhile, when a Ta foil covered the plasma electrode surface, it did not show an enhancement as large as that observed by evaporation [9]. Titanium (Ti) and Ti alloys also absorb hydrogen atoms at elevated temperature [10]. Thus, a thin foil of Ti could be placed on the surface of the plasma electrode if it improves the ratio of  $H^-$  ion current to electron current.

In this experiment, the negative hydrogen ion density near the plasma electrode ( $n_{H^-}$ ) is measured by the laser photodetachment method [11,12], and the measured density is correlated to the extracted  $H^-$  ion current ( $I_{H^-}$ ). The  $H^-$  ion current and the co-extracted electron current ( $I_{ext}$ ) are measured simultaneously by sweeping the bias potential applied to the plasma electrode [13], and the electron current is estimated to be equal to  $I_{ext}$  as the Faraday cup and the extractor are biased separately. The electron density ( $n_e$ ), electron temperature ( $T_e$ ) and plasma potential ( $V_p$ ) are determined from the Langmuir probe measurements.

## EXPERIMENTAL SETUP

A single filament serves as the cathode to sustain an arc discharge in a cylindrical ion source. Figure 1 shows a schematic diagram of the ion source chamber. The chamber has a diameter of 150 mm and a height of 200 mm. Connecting a turbo molecular pump and a rotary pump in series, ultimate vacuum pressure reaches  $5.0 \times 10^{-5}$  Pa in the ion source chamber. A stainless-steel plate with four pumping orifices of 12.7 mm diameter separates the main chamber and the manifold connected to the turbo molecular pump which stably keeps the  $H_2$  gas pressure of plasma production region at 0.5 Pa. Sixteen rows of samarium cobalt magnets equipped on the outside chamber wall forms a hexadecapole multi-cusp magnetic field. The chamber side wall has twelve ICF-34 flange ports aligned on three planes with four ports arranged to observe the axis of the chamber at right angles. A water cooling system protects permanent magnets from the discharge heating.

The filament dimensions are 0.5 mm in diameter and 90 mm long. A single filament is set at the bottom position of the chamber where the distance from the bottom flange is 45 mm. The filament is negatively biased at 80 V against the chamber wall to drive a DC plasma at 1 A discharge current. Figure 2 shows a diagram of the details of the extraction structure. A pair of permanent magnet forms the filter magnetic field, and creates a volume of low temperature plasma in front of the extraction hole. A 145 mm diameter, 2 mm thick stainless-steel plasma electrode (PE) is introduced into the chamber separated by 25 mm from the top flange. The PE has an extraction hole of 5 mm diameter. A floating electrode (FE), separated by 2 mm from the PE, has a center hole of 30 mm diameter and 1.5 mm thickness. The FE made of stainless-steel masks the PE surface to protect the PE surface from direct exposure to the plasma except the center 30 mm diameter region. A Ta or a Ti foil which has the area of  $50 \times 50 \text{ mm}^2$  and a thickness of 0.1 mm is attached between the PE and the FE as shown in Fig. 3. Electrons and negative ions are extracted by biasing the extraction electrode at 800 V electrical potential. The  $H^-$  ion current is measured by the Faraday cup also biased at 800 V with respect to the ion source chamber ground. A pair of permanent magnets on the top flange provides a magnetic field in the extraction region. The extraction electrode collects only the electron current,  $I_{ext}$  and the Faraday cup collects only the negative ion current,  $I_{H^-}$  because of the magnetic field present in the region between the extraction hole and the entrance of the Faraday cup; this field serves as the electron suppression field. An L-shaped 0.5 mm diameter 12 mm long Langmuir probe made of W is inserted into the top part of the chamber. The distance between the PE and the Langmuir probe is 12 mm.

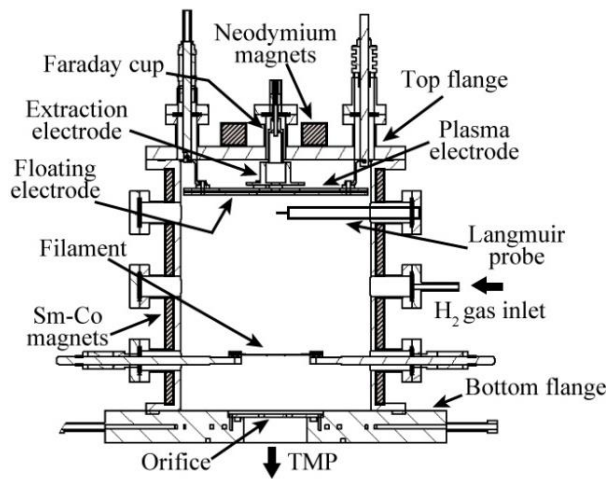


FIGURE 1. The diagram of the experimental setup.

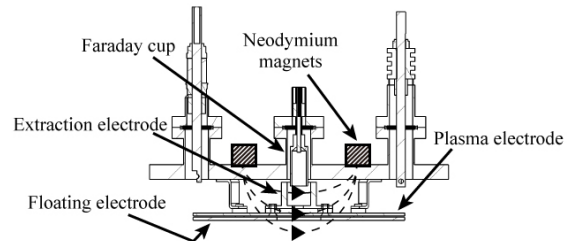


FIGURE 2. A diagram of the extraction system. Broken lines show magnetic field lines of force.

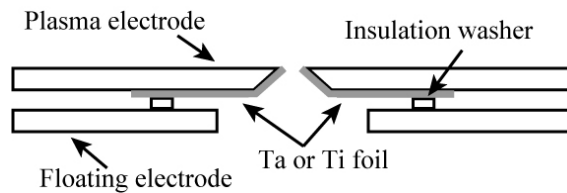
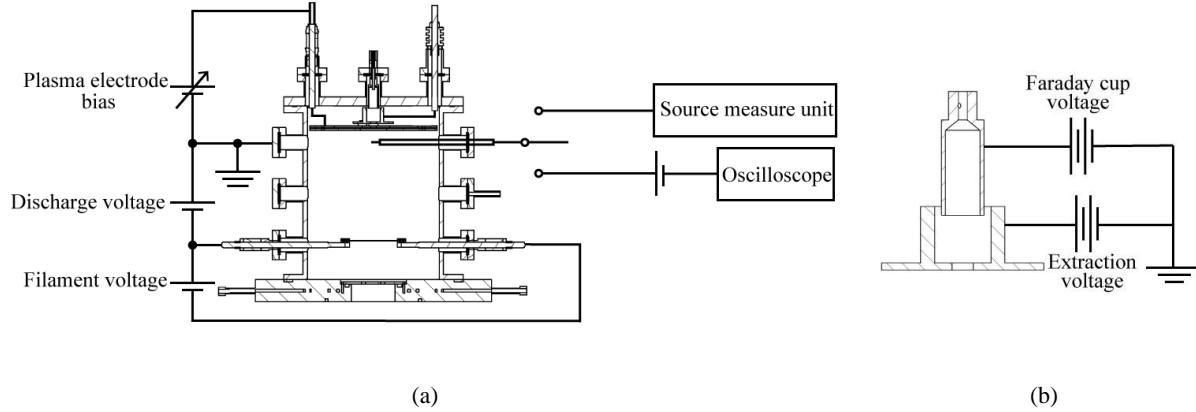


FIGURE 3. A schematic showing how to cover PE with a foil.

Figure 4 represents the schematic diagram of the electrical connection of the experimental system. Devices not shown in the figure include the current monitor of the Faraday cup high voltage power supply, the current monitor of the extraction voltage, and the current monitor of the plasma electrode bias. The location of the vacuum ionization gauge is at the center plane of the ion source chamber.

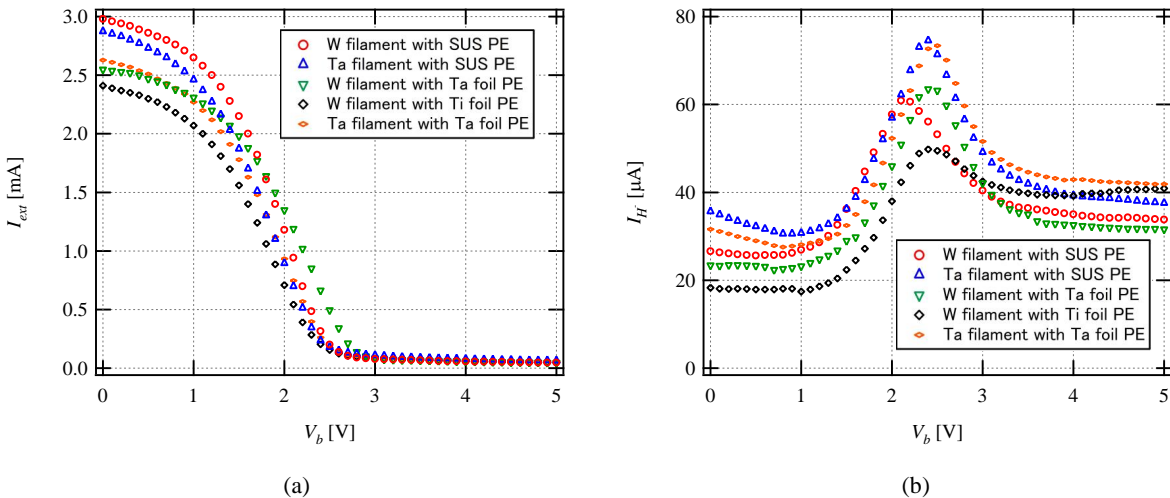


**FIGURE 4.** The schematic diagram of the experimental apparatus: (a) the overall view, (b) the details of the extraction system.

## RESULTS

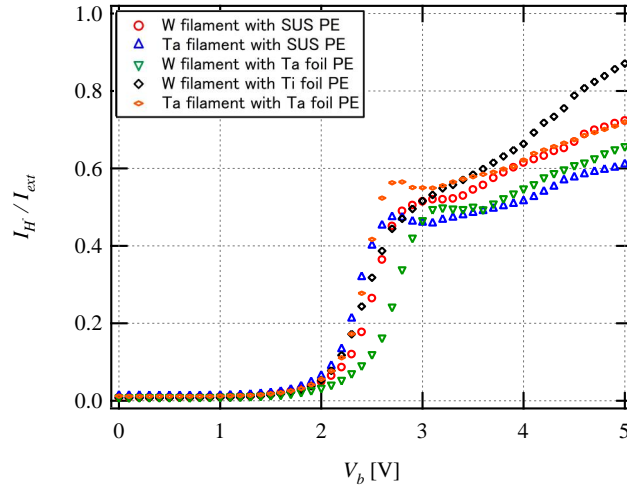
### Extracted $H^-$ Ions and Electrons from a Hydrogen Plasma

We conducted experiment by five patterns as follows; W filament with stainless steel (SUS) PE, Ta filament with SUS PE, W filament with Ta foil PE, W filament with Ti foil PE and Ta filament with Ta foil PE. Figure 5(a) shows the extracted electron current  $I_{ext}$ , and Figure 5 (b) shows the extracted negative hydrogen ion current,  $I_{H^-}$  as a function of PE bias voltage  $V_b$ .



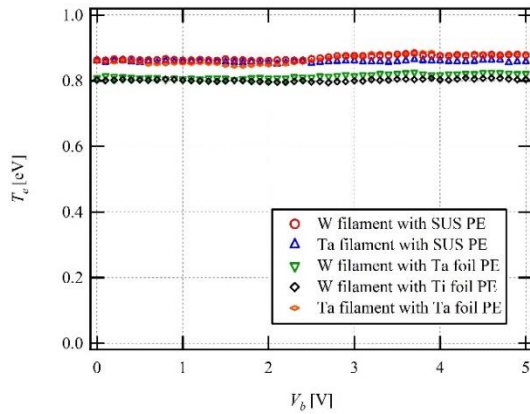
**FIGURE 5.** The effect of different hot cathodes and foil materials on PE for extracted  $H^-$  ion and electron currents versus PE bias voltage: (a) co-extracted electron current, (b)  $H^-$  ion current.

Figure 6 shows the ratio of  $I_{H^-}/I_{ext}$  as the function of PE bias voltage  $V_b$ . The peak value of  $I_{H^-}$  for the Ta filament operation was larger than that for the W filament operation but  $I_{ext}$  was also larger. Covering the PE with a Ta foil did not increase  $I_{H^-}$  while it decreased  $I_{ext}$  enhancing the ratio  $I_{H^-}/I_{ext}$ . Covering the PE with a Ti foil decreased both extracted  $I_{H^-}$  and co-extracted  $I_{ext}$ . Using a Ta filament as a hot cathode and covering the PE with a Ta foil showed the highest  $I_{H^-}/I_{ext}$  among the combinations tested in this experiment.



**FIGURE 6.** The effect of different hot cathodes and foils on PE on currents ratio of  $H^-$  ions and electrons versus PE bias voltage.

### Plasma parameters near the plasma electrode



**FIGURE 7.** Electron temperature versus PE bias voltage.

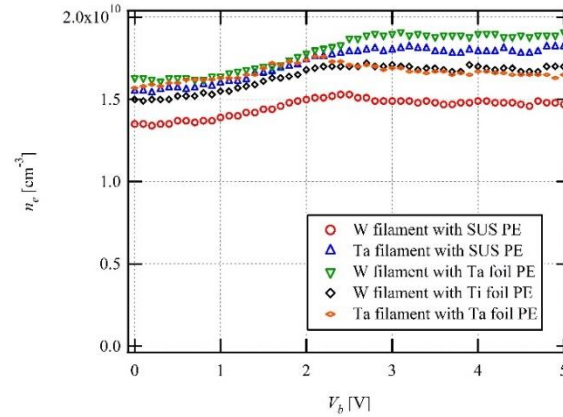


**FIGURE 8.** Electron density versus PE bias voltage.

Plasma parameters  $n_e$ ,  $T_e$  and  $V_p$  are obtained from  $I$ - $V$  characteristics of the Langmuir probe placed at the position 12 mm from the PE while scanning  $V_b$ . Figure 7 shows electron temperature  $T_e$  against  $V_b$ . For the two cases of the Ta foil and the Ti foil, W filament operation reduced the electron temperature compared with the stainless-steel PE. Meanwhile, the electron temperature of the plasma excited by Ta filament hitting a Ta foil did not show change from  $T_e$  of plasmas for stainless steel PE. Figure 8 shows the measured electron density  $n_e$  against  $V_b$ . The standard condition of stainless PE with the plasma excited with a W filament cathode showed the smallest density among the tested combination of the cathode and the PE surface materials. The PE surface

covered with a Ta foil showed a higher density of plasma excited by a W filament but the Ta filament did not increase  $n_e$  when it excited plasma in front of the Ta covered PE.

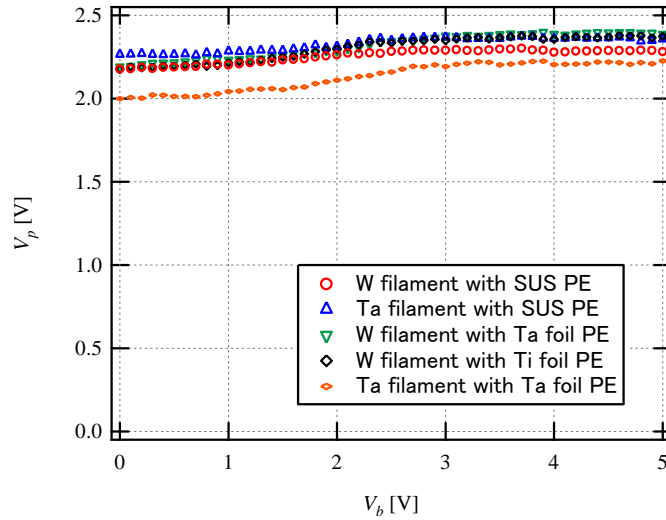


FIGURE 9. Plasma potential versus PE bias voltage.

As the probe was separated from the PE by 12 mm, no substantial correlation between the plasma potential  $V_p$  and the PE bias voltage  $V_b$  was observed as shown in Fig. 9. Among the tested combination of the filament and the PE surface materials, Ta PE surface in a plasma excited by the Ta filament had shown the smallest plasma potential.

### Negative hydrogen ion density

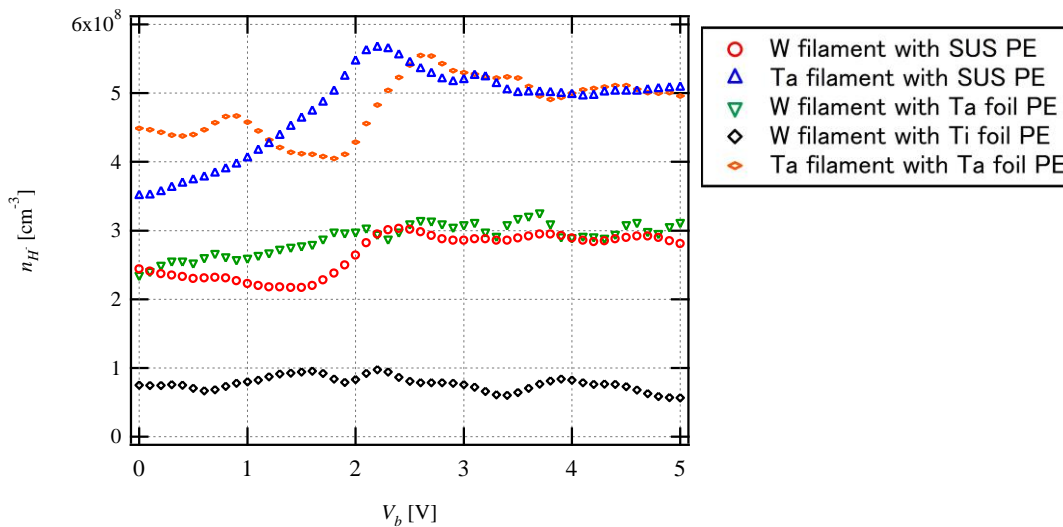


FIGURE 10. Negative hydrogen ion density  $n_{H^-}$  against PE bias voltage.

Negative hydrogen ion density was quantified by photodetachment method by biasing the probe at +12 V with respect to the chamber wall. As the local plasma potential was less than 2.5 V as shown in Fig. 9, this bias voltage is well within the electron saturation region. A 1064 nm laser pulse irradiated the area around the probe, and a rapid increase of electron saturation current was detected on the oscilloscope. This current jump was compared to the DC electron saturation current to determine the local  $H^-$  ion density. Figure 10 shows negative hydrogen ion density  $n_{H^-}$  against  $V_b$ . The result clearly shows that Ta filament increased the negative hydrogen ion density in the plasma near the PE for both stainless-steel and Ta used as the PE materials. When Ti is exposed to the plasma as the PE surface the negative ion density decreased down to 64% from the  $n_{H^-}$  of the normal operating condition with the W filament and stainless-steel PE. Covering the PE with a Ta foil did not change  $n_{H^-}$  substantially and it seems that the positive effect of Ta only appears as it is used as the material for a filament sustaining the discharge.

## DISCUSSION

The  $n_{H^-}$  plotted in Fig. 10 and the  $I_{H^-}$  in Fig. 5 (b) may not be directly compared as the 12 mm spacing exists between the PE surface and the probe tip. The filter magnetic field together with the electrostatic shielding by the floating potential seems to have detached the plasma in the vicinity of the extraction hole from the region measured by the probe. Still, the negative ion density near the extraction region plasma seems to show a weak peaking associated with the  $V_b$  bias, corresponding with the peak of  $I_{H^-}$ . In the meantime, the dependence of  $n_e$  upon  $V_b$  in Fig. 8 seems to show no relevance to  $I_{ext}$  vs  $V_b$  curve in Fig. 5 (a). The 12 mm distance may limit the penetration of the electrical potential from the PE to the region of the probe measurement. From Figs. 7 to 9, the plasma parameters do not show large differences, while substantial change in  $n_{H^-}$  was observed depending upon the filament materials and the materials of the PE surface. Namely, the plasma-PE surface interaction plays a decisive role in both  $n_{H^-}$ ,  $I_{H^-}$ , and  $I_{H^-}/I_{ext}$ .

Operation of the extraction system with the Ti foil covered PE had been tested for the first time to see, if the hydrogen adsorption effect on Ti can cause a characteristic behavior in  $I_{H^-}$  intensity. If the Ti PE surface reduces the density of hydrogen atoms near the extraction hole, the reaction rate of associative detachment ( $H^- + H^0 > H_2 + e^-$ ) can be reduced and more  $H^-$  ions can survive the transport from the plasma to the extraction hole yielding larger  $I_{H^-}$ . The results in Fig. 5(a) and Fig. 10 are against this speculation; the extracted  $I_{H^-}$  and local  $n_{H^-}$  are lower when the PE surface was covered with Ti. However, Ti also diminishes  $I_{ext}$  in Fig. 5(a) and at  $V_b$  higher than the plasma potential, Ti shows the largest  $I_{H^-}/I_{ext}$  ratio.

The  $H^-$  ion current did not increase by covering the surface of PE with a Ta foil, as can be seen on Figure 5(b). The fact that covering the PE with a tantalum foil does not increase  $I_{H^-}$  explains the observation of Stockli [14] who used an RF discharge, thus no filament, but implemented a tantalum foil on the plasma electrode. and did not observe any enhancement of  $I_{H^-}$ . The Ta covered PE surface reduced the  $I_{ext}$  as seen in the Fig. 5(a). Consequently, the Ta foil covered PE maximized the  $I_{H^-}$  to  $I_{ext}$  ratio under the operation with a Ta filament. The effect of reducing negative ion current with further decreasing electron current is similar to the observed result for a Ti covered PE.

## CONCLUSION

The extraction region plasma-PE surface interaction was found important through the experiments replacing the material of the foil covering the PE surface. While the higher density of  $H^-$  ions can be attributable to more efficient production of vibrationally/rotationally excited molecules by Ta filament, a Ta covered PE surface reduced the electron current like a Ti covered PE surface. Further investigation on which fundamental process is responsible to the observed reduction of the electron current will be made with an improved diagnostic system including an optical spectrometry.

## ACKNOWLEDGEMENTS

We thank Professor Martha Bacal for her useful discussion. This work has been supported in part by Japan Society for Promotion of Science KAKENHI No. 17H03512.

## REFERENCES

1. K. H. Berker, R. V. Pyle, J. W. Sterns, Nuclear Fusion, **15**, 249 (1975).
2. M. Bacal, Mamiko Sasao, Motoi Wada, Roy McAdams, Rev. Sci Instrum. **87**, 02B132 (2015).
3. R. Friedl, S. Cristofan, U. Fantz, AIP Conf. Proc., **2011**, 050009 (2018).
4. M. Sasao, R. Moussaoui, D. Kogut, J. Ellis, G. Cartry and M. Wada, Appl. Phys. Express **11**, 066201 (2018).
5. M. Bacal, A.A. Ivanov, M. Glass-Maujean, Y. Matsumoto, M. Nishiura, M. Sasao, M. Wada, Rev. Sci. Instrum. **75**, 1699 (2004).
6. S. Masaki, K. Maeshiro, K. Katsuyoshi and M. Wada, Plasma Fusion Res. **14**, 3401136 (2019).
7. M. Nishiura, M. Sasao, Y. Matsumoto, and M. Hamabe, Rev. Sci. Instrum. **73**, 949 (2002).
8. M. Bacal and M. Wada, AIP Conf. Proc., **1869**, 030025 (2017).
9. K. Maeshiro, M. Wada, S. Masaki, Proceedings of 34<sup>th</sup> ICPIG, PO16PM-027 (2019).
10. A. Lopez-Suarez, J. Rickards, R. Trejo-Luna, Int. J. Hydrogen Energy, **28**, 1107-1113 (2003).
11. M. Bacal and G. W. Hamilton, Phys. Rev. Lett. **42**, 1538 (1979).
12. M. Bacal, G. W. Hamilton, A. M. Bruneteau, and H. J. Doucet, Rev. Sci. Instrum. **50**, 719 (1979).
13. K. N. Leung, K. W. Ehlers, and M. Bacal, Rev. Sci. Instrum. **54**, 56 (1983).
14. M. Stockli, Private Communication with M. Bacal.